Journal of King Saud University – Science 33 (2021) 101364

Contents lists available at ScienceDirect

Journal of King Saud University – Science

journal homepage: www.sciencedirect.com

Original article

Synthesis, photophysical, cyclic voltammetry properties, and molecular structure study of novel (5,10,15,20-tetratolylphenyl porphyrinato)zinc (II) with pyrazine

Raoudha Soury [a,*], Khalaf M Alenezi [a], Ilona Turowska-Tyrk [b], Frédérique Loiseau [c]

[a] Department of Chemistry, College of Science, University of Hail, Ha'il 81451, Saudi Arabia
[b] Faculty of Chemistry, Wrocław University of Technology, WybrzeżeWyspiańskiego 27, 50-370 Wroław, Poland
[c] University of Grenoble Aples, Department of Molecular Chemistry, UMR CNRS 5250, ICMG-FR 2607, France

ARTICLE INFO

Article history:
Received 4 November 2020
Revised 22 January 2021
Accepted 3 February 2021
Available online 11 February 2021

Keywords:
Synthesis
Zn-porphyrin
Photophysical studies
Cyclic voltammetry properties
Solid-state structure

ABSTRACT

The precursor (5,10,15,20)-tetratolylporphyrin (H_2TTP) (**1**) and Zn(II) complex (5,10,15,20)-tetratolylporphyrinato)zinc(II) [Zn(TTP)] (**2**) have been synthesized and utilized to afford a novel complex (**3**) bearing pyrazine as fifth coordination site on axial position, i.e. (pyrazine)(5,10,15,20-tetratolylporphyrinato)zinc (II) hemi-pyrazine hemidichloromethane solvate [Zn(TTP) (pyz)]0.0.5(pyz.CH_2Cl_2). Photophysical, electrochemical and X-ray diffraction were investigated. The single-crystal X-ray analysis indicated that in complex (**3**) (**i**) Zn(II) ion is penta coordinated, (**ii**) slight displacement of Zn atom by −0.28 Å towards the axial ligand (pyrazine) and (**iii**) the crystal lattice is made up of two dimensional layers stabilised by C−H···Cg intra- and intermolecular interactions (Cg is the centroid of pyrrole ring). Optical absorption studies revealed a redshifted of the Soret (B) and Q bands of the Zn-porphyrins complexes. Contrarily, a hypsochromic shift of Q bands in emission spectra of the complexes is noted as compared to the H_2TPP. Lifetime of the electrons in (**1**–**3**) were determined and compared. Overall, this study would assist in understanding the impact of incorporation of pyrazine at the axial position on optical and electronic properties. Cyclic voltammetry (CV) was applied for the study of the electrochemical behavior of both (**2**) and (**3**) complexes in 0.2 M Tetra-n-butyl ammonium perchlorate (TBAP) solution in CH_2Cl_2. The results of electrochemical confirmed the potentials redox peaks shift more negative ca 60 mV to that ~~is~~ caused by the coordination of pyrazine ligand.

1. Introduction

Porphyrin and metalloporphyrin are π-conjugated macrocyclic scaffolds that are ubiquitously found in nature (Nath et al., 2016; Lu and Kobayashi, 2016). This class of compounds is known for its unique and tuneable photophysical properties (such as broad and intense absorption spanning visible region and colourful emission), high chemical and thermal stability (Sommer et al., 2011). Indeed, this is attributed to the planar and electron-rich four pyrrolic units connected *via* methylene unit (Jusélius and Sundholm, 2000). Besides, high rigidity, delocalisation of 22 π-electrons around the large ring system, and the presence of chemical modification sites (*meso* and β-positions) are added advantage with this class of chromophore. Owing to these features, a range of substituted porphyrins and their corresponding complexes have been reported (Lu and Kobayashi, 2016; Imahori et al., 2009; Chatterjee et al., 2016). Interestingly, many of them have shown potential candidateship for optoelectronic (Imahori et al., 2009; El-Nahass et al., 2014; Lind et al., 2009), sensing (Gujarathi, 2020; Park et al., 2013), catalysis (Barona-Castaño et al., 2016), bioimaging (Haque et al., 2017), and other intriguing applications (Haque et al., 2018).

It has been demonstrated that the energy levels, absorption/emission properties and applications can be significantly modulated by varying the substituents present at the periphery (*meso* and β-positions) and metal at the centre (Soury et al., 2018a, 2019; Chatterjee et al., 2016; El-Nahass et al., 2014). For example, it is found that the substituent present at *meso* position controls

* Corresponding author.
E-mail address: ra.soury@uoh.edu.sa (R. Soury).

Peer review under responsibility of King Saud University.

Production and hosting by Elsevier

https://doi.org/10.1016/j.jksus.2021.101364
1018-3647/

the catalytic activity of the complexes (Barona-Castaño et al., 2014). Similarly, when a suitable organic spacer is linked to the *meso* positions *via* alkynyl unit, electronic communication and photo-sensitization effect can be observed (Haque et al., 2018). In addition, a plethora of studies have demonstrated that photophysical properties of porphyrin and metalloporphyrin is a direct function of the spacer attached to it. Regarding the metals, it is found that the insertion of late transition metal like Zn(II) changes the symmetry of the free ligand and thus the optical properties (Gouterman, 1959). Also, the extent of shifting of the Q-bands has been related to the nature of the metal centre, the *meso* substituents and the porphyrin macrocycle undergoes non-planar distortion (Soury et al., 2018a, 2019, 2018b). During the literature survey, we noted that Zn(II) complexes bearing substituted porphyrin has already been reported (Lu et al., 2016; Chatterjee et al., 2016). However, those bearing pyrazine as fifth coordination site is yet to be explored (Chart 1).

Therefore, it would be interesting to see the effects of insertion of Zn(II) cation and the axial ligands in the *meso* porphyrin on the electronic, redox, structural and photophysical properties. Based on these notions, we herein report the synthesis, characterization, optical and dielectric properties of a free base (5,10,15,20)-tetrato lylporphyrin (H_2TTP) (**1**) and corresponding Zn(II) complexes (5,10,15,20)-tetratolylporphyrinato)zinc(II) [Zn(TTP)] (**2**) and hemi-pyrazine hemidichloromethane solvate [Zn(TTP) (pyz)]0.0.5 (pyz.CH_2Cl_2) (**3**). The IR and ^{1}H NMR, optical and emission spectroscopy, as well as Electrospray mass spectrometry are used to characterize ligands as well as complexes. The structure of one of the complexes (**3**) is also evidenced by single crystal X-ray molecular structure.

2. Experimental

2.1. Materials and methods

2.1.1. Materials

The solvents and reagents are of grade quality and used as received.

2.1.2. Preparation of H_2TTP (1) and [Zn(TTP)] (2)

Ligand H_2TTP (**1**) and Zn(II) complex [Zn (TTP)] (**2**) were prepared following the procedure reported in literature (Adler et al., 1967; Hoard and Smith, 1975). The structure of the synthesized materials was confirmed using state of the art analytical technique prior to use for subsequent steps.

2.1.3. Synthesis and crystallization of [Zn(TTP)(pyz)]0.0.5(pyz.CH_2Cl_2) (3)

[Zn(TTP)] (**2**) (25 mg, 0.020 mmol) and pyrazine (90 mg, 1.125 mmol) were dissolved in 5 ml of dichloromethane (CH_2Cl_2). A purple to green–blue colour changes of the mixture was observed. Dark purple crystals of complex (**3**) were acquired by n-hexane slow diffusion in the CH_2Cl_2 solution. (in 89% yield). Anal. Calc. For [Zn(TTP)(pyz)]0.0.5(pyz.CH_2Cl_2): $C_{53.25}H_{41.5}N_{6.5}Cl_{0.5}Zn$ (855.6 g/mol).C, 6.27; H, 4.80; N, 75.97%. Found: C, 6.31; H, 4.76; N, 75.81%. UV–Vis [CH_2Cl_2, λ_{max} in nm (logξ)]: 425 (5.47), 560 (4.27), 604 (4.03). ^{1}H NMR ($CDCl_3$, 300 MHz): δ (ppm) = 8.89 (S, 8H, H_β), 8.04 (d, 8H, $H_{o,o'}$); 7.53(d, 8H, $H_{m,m'}$) ; 6.35(d, 4H, H_1) ; 2.3(s, 12H, $CH_{3\text{-Mésithy}}$. IR (cm^{-1}): 3020–2930: ν[CH(porph)]; 952: δ[CCH(porph)];700: δ [CC(phenyl porphy)], 3130: ν[CH(pyz)], 1500: ν[CN(pyz)].

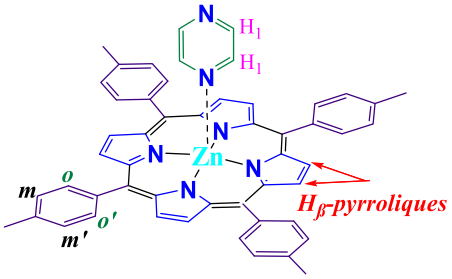

Chart 1. Chemical structure and numbering scheme for complex (**3**).

2.2. Characterization

2.2.1. ^{1}H NMR, absorption and emission properties

The Bruker 300 Ultrashield spectrometer was used to perform the room temperature^{1}H NMR spectra. UV–vis spectra and titration were obtained by using WinASPECT PLUS. Emission spectra were also detected on Horiba Scientific Fluoromax-4 spectrofluorometer. The 1 cm path length quartz cuvettes were used to analysed samples. Emission measurements were observed after irradiation at λ = 400 nm observed by the second harmonic of a titanium laser with a replication rate of 8 MHz. To detect the decay acquisition, Fluotime 200 (AMS technologies) is used with a GaAs microchannel plate photomultiplier tube (Hamamatsu model R3809U-50) followed by a Picoquant temporal correlation single photon counting system (PicoHarp300). The eventual time resolution of the setup is proximate to 30 ps. Picoquant-FLUOFIT software, was used to accomplish luminescence decays. The optically diluted method was used to detect quantum emission efficiencies in CH_2Cl_2 solutions at 25 °C (Yang et al., 1999). [Zn (TPP)] in a dichloromethane solution equilibrated in air was used as a quantum yield standard (Φ = 0.031). Here are the experimental uncertainties: 20% for the emission lifetimes; 2 nm and 5 nm for the absorption maxima and the emission maxima, respectively.

2.2.2. Electrochemistry

Cyclic voltammetry (CV) experiments were carried out with a CH-660B potentiostat (CH-instrument) at room temperature under an argon atmosphere (argon stream), using three-electrode electrochemical cell, in a standard one-compartment. Tetra-n-butylammonium perchlorate (TBAP) was utilized as a support electrolyte (0.2 M) in dichloromethane (CH_2Cl_2) after distillation with calcium hydride under argon. An automatic ohmic drop compensation procedure was systematically realized prior to recording the CV data in electrolytic solutions containing the studied compound at a concentration ~10-3 M. CH-instrument vitreous carbon (Φ = 3 mm) working electrodes were polished with 1 μm diamond paste before each recording. As a reference electrode was used the redox couple Ag/Ag^+ (10^{-2} M + TBAP 0.2 M in CH_2Cl_2).

2.2.3. X-ray characterisation

Data collection for compound (**3**) were performed at 298 K, the data are obtained by the Xcalibur, Sapphire 2, Eos, Gemini ultra. The monochromatized, λ = 0.71073 Å, MoKα graphite radiation was used. The data intensity were detected via a narrow-frame procedure. The CrysAlis RED (Oxford Diffraction, 2010) software was used to obtain the unit cell parameters, reflections are scaled and corrected for absorption (Oxford Diffraction, 2010). SIR-2004 via a direct method was used to elucidate the trial structure (Altomare et al., 1994). The final structural refinement was made against F^2 data with the program SHELXL-97 (Sheldrick, 2008).

3. Results and discussion

3.1. Optical absorption investigation

The UV–visible spectra of the compounds (**1**–**3**) were collected in dichloromethane at a concentration of ca10^{-6}M and 10^{-5} M, for the intense band (Soret band) and other bands (Q-bands), respectively (Fig. 1). The λ_{max} values of these species were compared to other *meso*-porphyrins and Zn(II)-metalloporphyrins and are gathered in Table 1.

Fig. 1 shows the absorption spectral changes of complexes (**1**–**3**).We noticed; (**i**) the reduction of the number of Q bands of low intensity from four (between 515 and 645 nm) to two bands (between 550 and 600 nm) on going from the free porphyrin (**1**) to complexes (**2**–**3**). This reduction in number of bands can be attributed to the change in symmetry (D_{2h} for free ligand vs D_{4h} for Zn-complexes) (Gouterman et al., 1959; Sharma et al., 2019); (**ii**) bathochromic shift of the values of λ_{max} of the soret and Q bands for (**2**–**3**) complexes are compared to the free base porphyrin. The shifts are 4 nm and 45 nm for the soret and Q-bands, respectively. This is supported by the earlier reported works (Soury et al., 2018a, 2019, 2018b).

3.2. Optical gap

The optical band gap is a fundamental property that characterize semicondutors physics. Fig. 2 depicts the optical band gap $E_{op\text{-}gap}$ of the ligands and complexes and are determined using the Tauc plot method (Tauc et al., 1966; Polat et al., 2020). As it is clear from the Fig. 2, the straight line portion of $(\alpha h\upsilon)^2$ *vs* photon energy ($E = h\upsilon$) plot until null absorption.

The $E_{op\text{-}gap}$ values of (**1**–**3**) compounds are 1.885, 2.019 and 2.036 eV, respectively. Notably the E_g $E_{op\text{-}gap}$ of free base is at higher value than that of the Zn(II)-metaloporphyrins and are close to 2.00 eV. It is noteworthy that the optical gap does not change significantly for the studied complexes, but their low optical gap could be suitable for potential use in the development of new opto-electronic organic semiconducting materials and related compounds.

3.3. Titration

Zn(II)-porphyrin are known to bind *N*-donors (imidazole, pyridine etc) through axially and forming five-coordinated complexes (Lin et al.,2002), with association constant (K_{ass}) in the range of 10^4 (Flamigni et al., 2006). In this work, we titrated complex (**2**) with a monodentate pyrazine ligand and change was monitored using UV/vis spectroscopy (porphyrin concentration values are: 10^{-6} M, 10^{-5} M for soret band and Q bands, respectively. Thepyrazine concentration values are: 10^{-4}, 10^{-3}, 10^{-2}, 0.1 and 0.2 M). Fig. 3, shows a typical change observed for (**3**) upon addition of pyrazine. The addition of incremental amounts of pyrazine to the solution of the second compound **(2)** induces: (**i**) colour change from purple to green (**ii**) the soret and Q-bands are considerably red-shifted (Lin et al., 2002) by 5 nm and 10 nm, respectively. This red-shift was complemented by forming a new compound 1:1 (pyrazine: [Zn(TTP)]) binding stoichiometry (Paul et al., 2003) (**iii**) the appearance of a sharp isobestic points around 424 nm and 580 nm-590 nm for the soret band and Q-bands, respectively.

These results indicate equilibrium between pyrazine and Zn(II) in compound (**2**). Titration data are determined to calculate the value of the association constant K_{ass} using the fitting procedure provided by the program GWBASIC. The value of binding constant in this study was found to be 1.5×10^3 M^{-1}, which is quite lower for Zn(II)-porphyrin bearing 4,4′-byp, 1-methyl-imidazol and 2-methyl-imidazole as axial fragment. This is most likely due to the strong basicity of the pyrazine donor (Soury et al., 2018a, 2019, 2018b; Flamigni et al., 2006; Paul et al., 2003). Spectroscopic data for Zn-complex are summarized in Table 1, along with some porphyrinic species with N-donor axial ligands.

3.4. Photoluminescence studies

Porphyrins and related compounds are known to exhibit two types of emission: (a) high energy and a strong transition to the second excited (S2 → S0 transition state) between 380 and 440 nm called Soret or bands . Such types of bands are comparatively rare, and (b) low energy and a weak transition (Q bands), which are assigned to the S1 → S0 transitions. The Q(x,y) are designated as bands, where "x" is the vibrational quantum number in the electronically excited state (S1) and "y" in the electronic

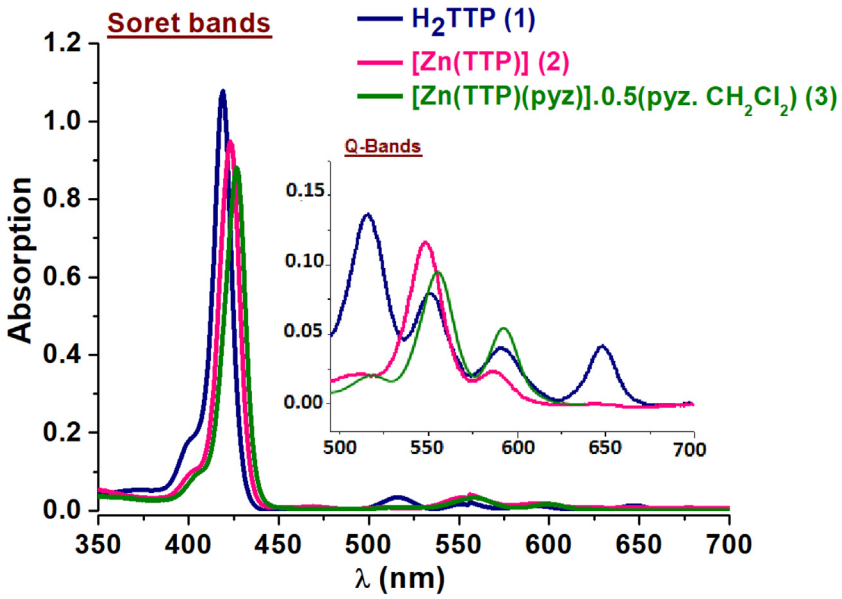

Fig. 1. UV–Vis spectra in dichloromethane of (**1**–**3**) compounds.

Table 1
UV–Vis data of H_2TTP, [Zn(TTP)], [Zn(TTP)(pyz)]0.0.5(pyz.CH_2Cl_2) and other related systems.

Porphyrin/Metalloporphyrin	Soret band λ (nm) (logε)	Q bands λ (nm) (logε)	Eg (eV)	Log K_{ass}	Ref.
H_2TTP[a] (**1**)	417 (5.95)	515 (5.82) 553 (4.28) 598 (4.17) 646 (4.10)	1.88	–	C.W
[Zn(TTP)][a] (**2**)	420 (5.75)	550 (4.31) 593 (3.86)	2.03	–	C.W
[Zn(TTP)] [a]	420 (-)	549, 588	–	–	[Kim and Shin, 2003]
Zn(TTP)(pyz)]0.0.5(pyz.CH_2Cl_2)[a] (**3**)	425 (5.47)	560 (4.27) 604 (4.03)	2.01	3.01 ± 0.2	C.W
[Zn(TTP)(4,4′-bpy)] [a]	428 (5.71)	562 (4.26) 602 (4.04)	2.02	5.14 ± 0.2	[Soury et al., 2018b]
[Zn(TTP)(mbpy ~ py)][c]	428 (-)	563 (-), 603 (-)	–	–	[Kim and Shin, 2003]
[Zn(TPP)(1-MeIm)][d]	428 (-)	564 (-) 604 (-)		5.3 ± 0.2	[Paul et al., 2003]
[Zn(TPP)(2-MeIm)] [d]	428 (-)	564 (-) 604 (-)		5.4 ± 0.2	[Paul et al., 2003]

[a]*in dichloromethane,* [b]*in toluene,* [c]*:mbpy ~ py = N-methyl- 2,2′-bipyridinium ~ pyridine,* [d] *in cyclohexane, 1-MeIm: 1-methyl-imidazole and 2-MeIm : 2-methyl-imidazole.*

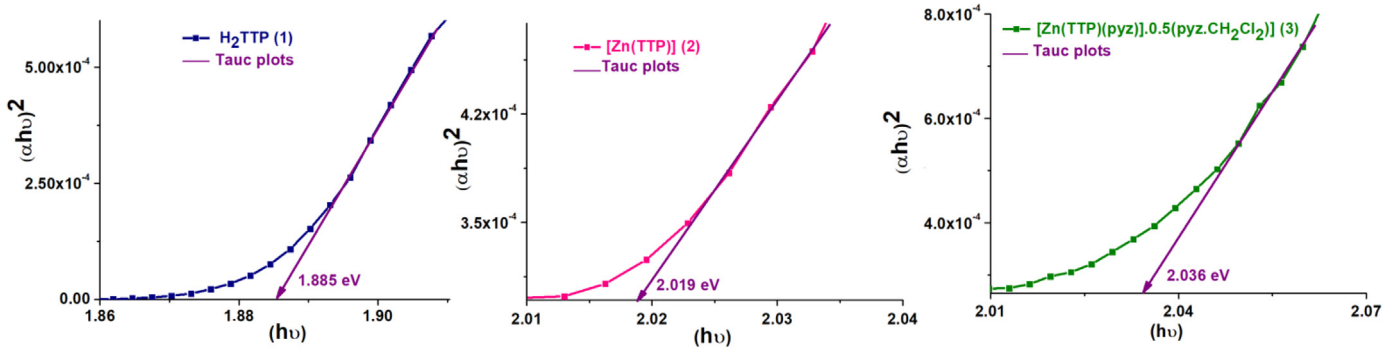

Fig. 2. Plotsof $(\alpha h\upsilon)^2$ vs photon energy E of (**1**–**3**) compounds. α is the absorption coefficient.

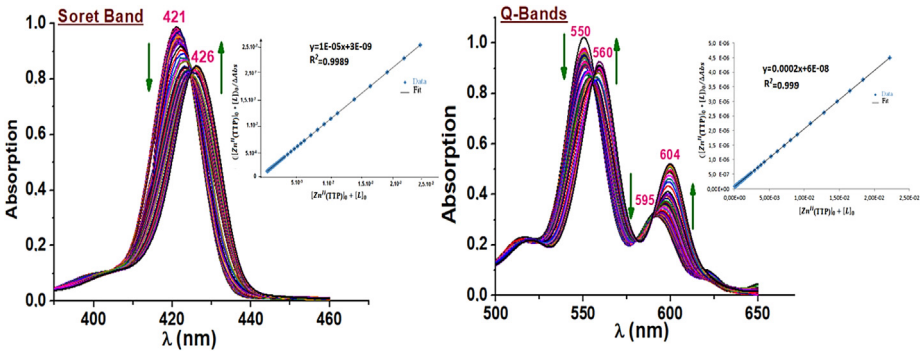

Fig. 3. UV–visible data for comlex (**2**) upon adding pyrazine showing left the Soret band shift 10^{-6} M in CH_2Cl_2.The changes around 426 nm with a 1:1 fit (0–5000 equiv.), are presented in the inset. The left side of the Figure showed the Q bands shift 10^{-5} M in CH_2Cl_2. The changes around 560 nm with a 1:1 [Zn(TTP)]/pyrazine fit, are presented in the inset. The study was carried out at 298 K in dilute dichloromethane solution.

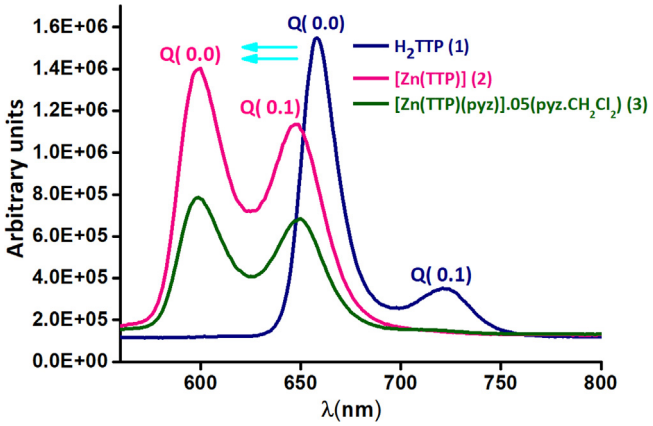

Fig. 4. The emission spectra of (**1**–**3**) species. The spectra are obtained in CH_2Cl_2, having almost10^{-6} M concentration.

ground state (S0). Hence, the individual bands correspond to the (0,0) and (0,1) transitions with respect to vibrational states (Fig. 4). As shown in Fig. 4, major hypsochromic shift about ca 50 nm in the Q (0,0) band and about ca 70 nm in the Q (0,1) band are between the free base porphyrin H_2TTP and the zinc porphyrins. The Q (0,0) emission bands of [Zn(TTP)] and the Q (0.1) emission bands of [Zn(TTP)pyz] 0.5(pyz.CH_2Cl_2) wavelengths are around 600 nm and 648 nm, respectively.

The decrease of the value of the fluorescence quantum yields (Φ_f): (Φ_f)(H_2TTP) = 0.045 > (Φ_f) ([Zn(TTP)] = 0.039 > (Φ_f) ([Zn (TTP)(pyz)] 0.5(pyz.CH_2Cl_2) = 0.030 are caused by the insertion of the zinc metal on the free-base porphyrin and the adding of the pyrazine as a axial ligand. The values of fluorescent lifetime of (**1**–**3**) compounds are 7.9, 1.6 and 1.6, respectively. The (τ_f) of H_2TTP is remarkably greater than those of the zinc-porphyrins complexes (Kim and Shin, 2003; Soury et al., 2018b; Oberda et al., 2013). The fluorescence τ_f depends on the insertion of the zinc metal, unaffected by the nature of the axial ligand.

3.5. X-ray crystallography of complex 3

The crystal was grown by slow diffusion of non-solvent (hexane) in solvent (dichloromethane). Key bond parameter data were listed in Table 2. The complex crystallizes in the monoclinic system (space group C 2/c). The parameters of the unit cell are a = 43.0761 (17)Å, b = 9.44945(19) Å, c = 24.3292(11) Å, β = 121.806(2) °, V = 8416.6 (8) Å and Z = 8. The asymmetric unit is composed of one [Zn(TTP)(pyz)] complex, one half pyrazine molecule and one half dichloromethane molecule. Fig. 5a, represents the molecular structure of [Zn(TTP)(pyz)] complex, the zinc metal is coordinated to the four nitrogen atoms of the porphyrinato core ring and the nitrogen atom of the pyrazine axial ligand, forming a distorted square-based pyramid as coordination polyhedron for zinc(II).

$^{a}: R_1 = \sum||F_o|-|F_c||/\sum|F_o|$. $^{b}: wR_2 = \left[\sum w(F_o^2-F_c^2)^2/\sum w(F_o^2)^2\right]^{1/2}$.

Zn(II) cation is coordinated to the four nitrogen atoms of the porphyrin ring with average equatorial distance value (Zn-Np) of 2.061 (2) Å and the nitrogen N5 atom of the pyrazine axial ligand with the Zn-N(pyridyl) bond length value of 2.203(2) (Å). The dihedral angle (Φ) between the "N_p-M−N_L" plan (N_p is the closest pyrrole nitrogen atom and N_L is the N atom of the pyrazine ligand axial) and the pyridyl plane of the axial ligand is 28.49 (2)° and the value of the dihedral angle between the pyrazine and the porphyrin core is 84.63(5)°. As shown in Fig. 5b, the formal diagram of the porphyrinato core of complex (**3**), where the metal is displaced by −0.28 Å toward the pyrazine axial ligand. This diagram shows that (**3**) presents a moderate *ruffling* (*ruff*) and doming deformations. The first deformation is indicated by the displacement of the *meso* carbons above and below the porphyrin mean plane (Jentzen et al., 1998). The *doming* (*dom*) deformation is often observed in five-coordinate complexes when the axial ligand causes a displacement of the metal center out of the mean plane, and the nitrogen atoms are also displaced toward the axial ligand (Scheidt and Lee, 1987).

In the crystal structure of the title compound [Zn(TTP)(pyz)] molecules are connected with each other in such way as to make a pair of layers, parallel to [0 1 0] direction, which are parallel to other pairs with an interlayer distance of 8.170 Å, while layers

Table 2
Crystal and refinement data of [Zn(TTP(pyz)] 0.5(pyz.CH_2Cl_2) (**3**).

Parameters	Complex (3)
CCDC	1,834,753
Empirical formula	$C_{53.25}H_{41.5}N_{6.5}Cl_{0.5}Zn$
Formula weight	855.6
Cryst. Sym	Monoclinic
Space group	C 2/c
a(Å)	43.0761(17)
b(Å)	9.44945(19)
c(Å)	24.3292(11)
β (°)	121.80(6)
V (Å^3)	8416.6(8)
Z	8
ρ_{calc} (g/cm^3)	1.056
μ (mm^{-1})	0.662
Max./min. trans.	0.944/ 0.753
F(000)	3560
Crystal size (mm^3)	0.55 × 0.46 × 0.11
T (K)	298
Θ range (°)	3.162–26.00
Limiting indices	$-53 \le h \le 53$,$-11 \le k \le 11$, $-30 \le l \le 30$
Reflec. collec/unique	32,187 / 8258
Parameters	575
S [Goodness of fit]	1.056
R_1^a, wR_2 [Fo > 4σ(Fo)]	R_1 = 0.047, wR_2 = 0.139
R_1, wR_2^b [all data]	R_1 = 0.060, wR_2 = 0.144
Min./max. res. (eÅ^{-3})	0.558 and −0.716

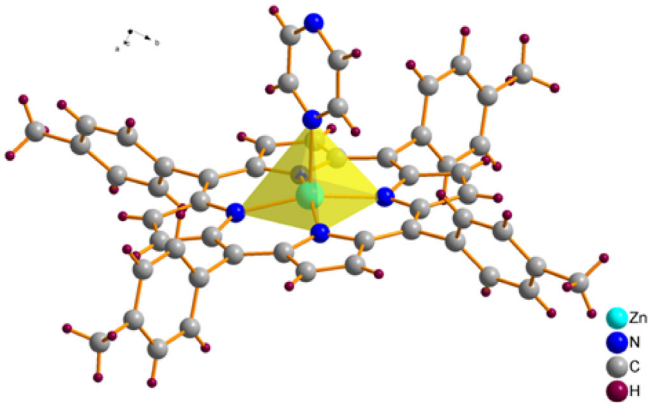

Fig. 5a. Molecular structure of [Zn(TTP(pyz)].

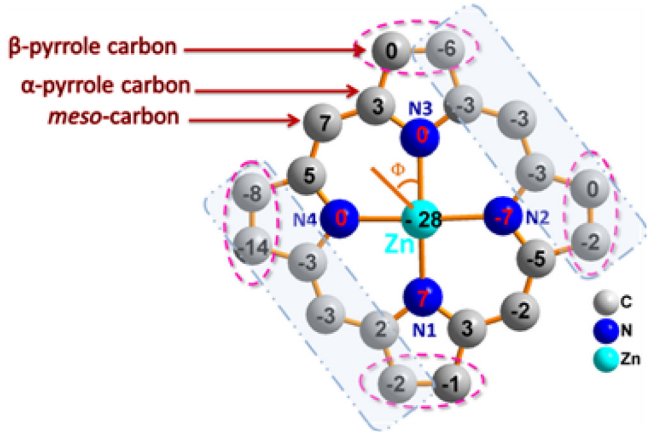

Fig. 5b. Formal diagram of the porphyrnato core of complex (**3**) illustrating the displacements of each atom from the 24-atoms core plane in units of 0.01 Å. Orientation of the pyz ligand vis-à-vis of the nearest N atom of the porphyrin ring (Φ dihedral angle) is also shown.

are spaced apart with 8.160 Å (Fig. 5c), where each 2D chain is stabilized by weak C–H···Cg intermolecular interactions.

Within a layer, the linkage of (**3**) is accomplished by two weak C-H…Cg intermolecular interactions between the carbon atom C47 and C29 of a phenyl ring of one TTP porphyrinate and the centroide Cg2 and Cg4 of a pyrrole ring of an adjacent [Zn(TTP)(pyz)] molecule and vice versa. The C47—H47···Cg2 and the C29—H29…Cg4 π intermolecular interactions are 3.469(4) Å and 3.444 (4) Å, respectively (Fig. 5d).

As can be seen from Fig. 5e, the presence of voids with radius of 1.2 Å and a grid of 0.7 Å are located between the 2D layers.

3.6. Cyclic voltammetry

The electro-oxidation of [Zn(TTP))] (**2**) and [Zn(TTP)(pyz)]0.0.5 (pyz·CH_2Cl_2) (**3**) were studied using cyclic voltammetry in 0.2 M Tetra-n-butyl ammonium perchlorate (TBAP) solution in CH_2Cl_2. All the experiments were carried under argon at vitreous carbon electrode at room temperature. The onset potentials that are quoted versus Ag/AgCl are given in the Table 3. The cyclic voltammetry of [Zn(TTP)] exhibits two successive reversible one-electron oxidation processes (Table 3). The two steps are obtained at potentials $E_{1/2}$ = 0.91 and.1.29 V versus Ag|AgCl that formally correspond to the first and second porphyrin ring oxidation. The cyclic voltammetry of complex (**3**) is shown in Fig. 6. The behavior is similar to that of [Zn(TTP)] and the both reversible one-electron waves

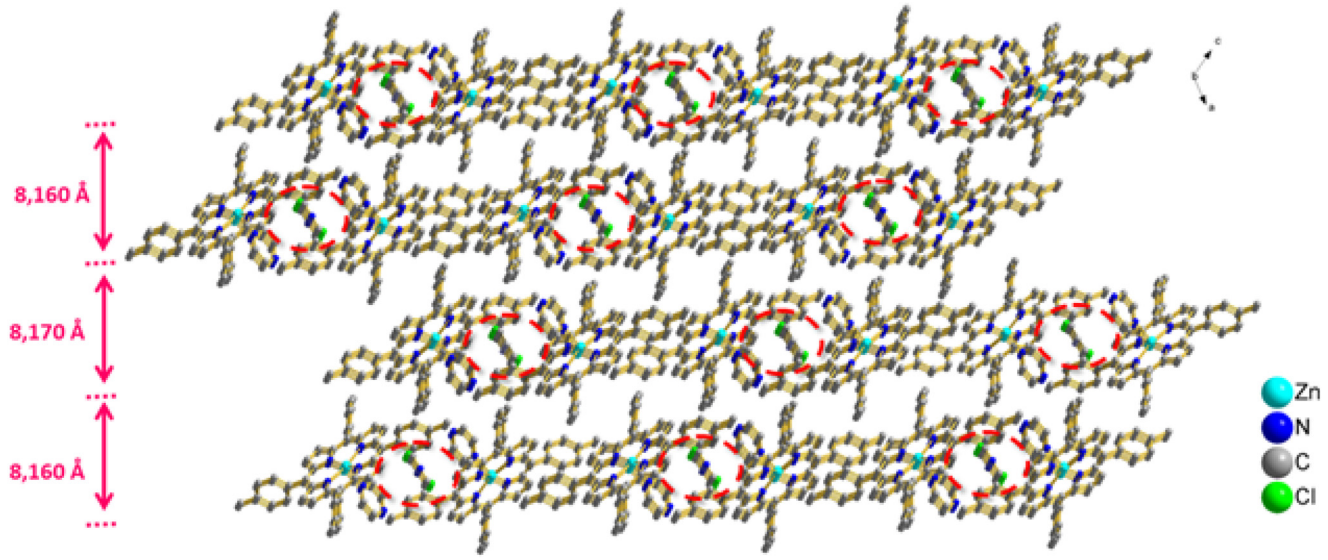

Fig. 5c. The packing of (**3**) viewed along the *b* axis showing the two-dimensional superstructure formed by pairs of layers containing the pyrazine free molecules.

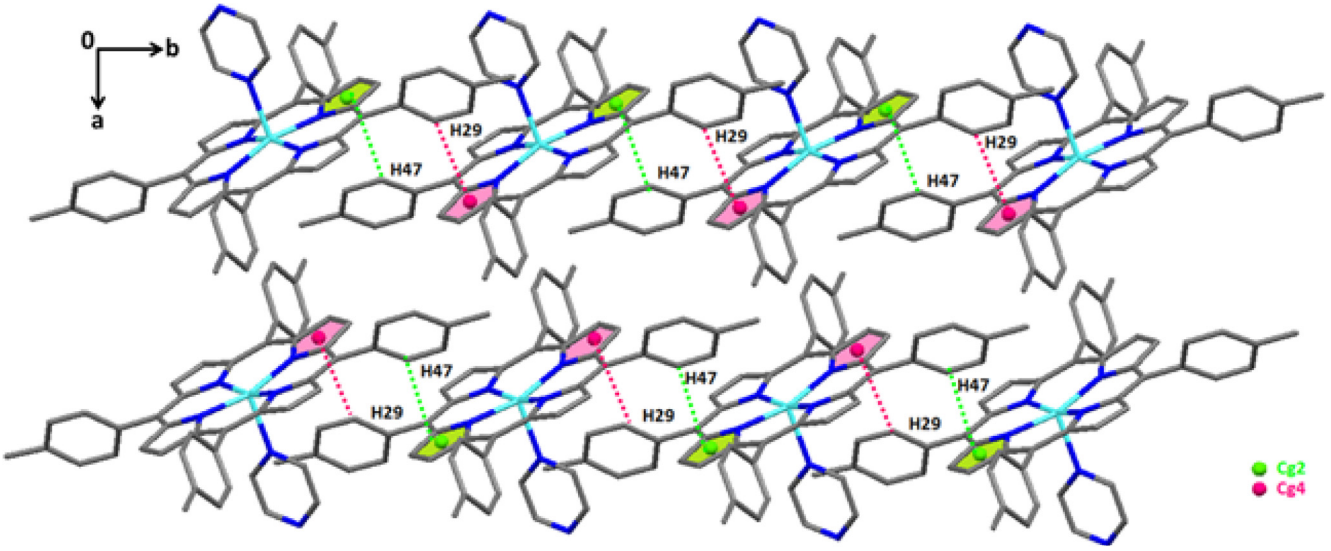

Fig. 5d. Drawing representing of the C47—H47···Cg2 and the C29—H29...Cg4 π intermolecular interactions in complex (**3**).

appears at $E_{1/2}$ = 0.84 and 1.23 V versus Ag|AgCl. Clearly, the addition of pyrazine coordinating group on the metal center cause a slightly shift (60 mV) to the more negative potentials comparing to [Zn(TPP)]. The electroreduction of both (**2**) and (**3**) complexes was examined under the same conditions. The results are shown in Fig. 6. The cyclic voltammetry of [Zn(TTP)] presents successive quasi-reversible reduction peaks at potential $E_{1/2}$ = − 1.22 V and an irreversible wave at Ep = − 1.34 V, whereas [Zn(TTP)(pyz)]0.0.5(pyz·CH_2Cl_2) shows a shift to the more positive reduction peaks (60 mV) that is caused by the coordination of pyrazine group. It fact, the two waves appears at $E_{1/2}$ = − 1.29 V and − 1.4 0 V vs. Ag|AgCl. It is worth mentioning that the second reduction wave of both (**2**) and (**3**) complexes exhibits a clear 2e reduction that could be a mix between Zn and porphyrin ligand reduction.

4. Conclusion

In this research article,the *meso*-porphyrin H_2TTP (**1**), [Zn(TTP)] (**2**) and a novel pyrazine-zinc-porphyrin [Zn(TTP)(pyz)]0.0.5(pyz·CH_2Cl_2) (**3**) are synthesized and characterized. Photophysical studies indicated that four and five coordinated Zn(II) complexes possess markedly different absorption and emission properties. However, the fluorescence values of the free base porphyrin H_2TTP is found to be higher than Zn(II) complexes. Titration experiment indicated equilibrium between pyrazine and Zn(II) in [Zn (TTP)] complex with moderate association constant (K_{ass}) values. In solid-state for compound **(3)**, Zn atom is five-coordinated with the pyrazine as an axial ligand. Moderate ruffling distortion and doming deformations are exhibited by porphyrin core. The supramolecular structure is formed with a two-dimensional chain, pairs parallel to the b axis in which each 2D chain is stabilized by weak intermolecular interactions C-H... Cg (The Cg is the centroid of pyrrole ring). In addition, this measurement is also suggestive of occurrence of electron transfer. The fact that the complexes (**2**) & (**3**) have high Eg values (≥2 eV), they could be used as component in semiconducting devices. Electrochemical properties of both (**2**) and (**3**) complexes were studied using cyclic voltammetry. The results showed the redox potentials of [Zn(TTP)(pyz)]0.0.5(pyz·CH_2Cl_2) ca 60 mV negative of the [Zn(TTP)] that is caused by the coordination of pyrazine axial ligand.

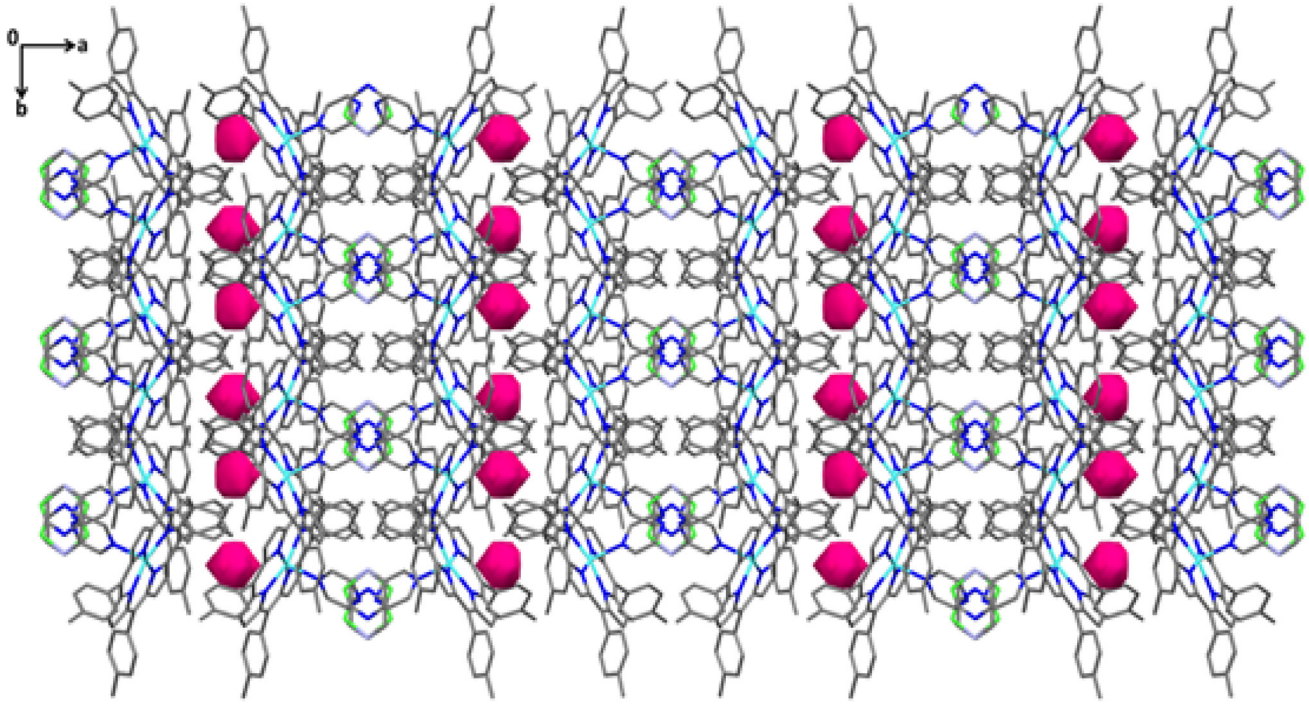

Fig. 5e. Packing diagram of (**3**) showing voids (represented in purple) calculated for a ball radius of 1.2 Å and a grid of 0.7 Å.

Table 3
Oxidation and reduction potentials (V vs Ag/AgCl) in CH_2Cl_2 containing 0.2 M (TBAP).

Complex	Oxidation		Reduction	
	$^1E_{1/2}$	$^2E_{1/2}$	$^1E_{1/2}$	^2E_p
[Zn(TTP)] (2)	0.91	1.29	−1.22	−1.34
[Zn(TTP)(pyz)]0.0.5(pyz·CH_2Cl_2) (3)	0.84	1.23	−1.29	−1.40

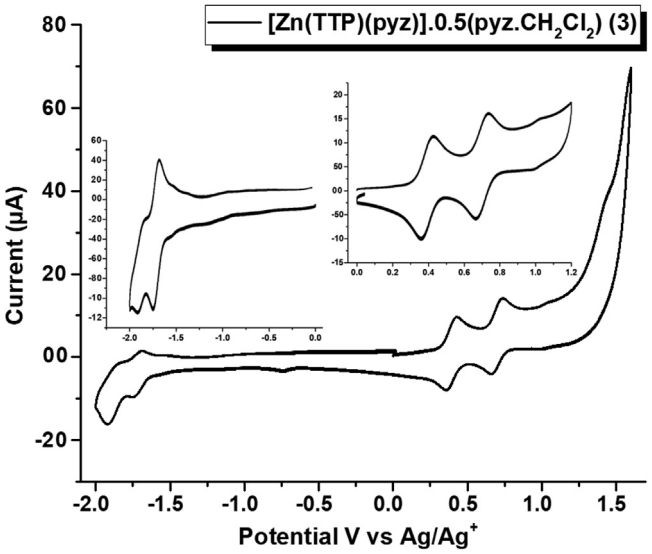

Fig. 6. Electro-oxidation and reduction of [Zn(TTP)(pyz)] in 0.2 M (TBAP) at RT in CH_2Cl_2. Scan rate = 0.1 V/s.

Acknowledgments

Dedicated to the memory of Professor Mohamed Salah Belkhiria (1951–2017) and Dr. Yassine Belghith (1982–2014), University of Monastir, Tunisia.

References

Adler, A.D., Longo, F.R., Finarelli, J.D., Goldmacher, J., Assour, J., Korsakoff, L., 1967. A simplified synthesis for meso-tetraphenylporphine. J. Org. Chem. 32, 476–476.
Altomare, A., Cascarano, G., Giacovazzo, C., Guagliardi, A., Burla, M.C., Polidori, G., Camalli, M., 1994. SIRPOW. 92–a program for automatic solution of crystal structures by direct methods optimized for powder data. J. Appl. Cryst. 27 (3), 435–436.
Barona-Castaño, Juan, Carmona-Vargas, Christian, Brocksom, Timothy, de Oliveira, Kleber, 2016. Porphyrins as catalysts in scalable organic reactions. Molecules 21 (3), 310. https://doi.org/10.3390/molecules21030310.
Chatterjee, Tamal, Shetti, Vijayendra S., Sharma, Ritambhara, Ravikanth, Mangalampalli, 2016. Heteroatom-containing porphyrin analogues. Chem. Rev. 117 (4), 3254–3328.
El-Nahass, M.M., Farag, A.A.M., Abu-Samaha, F.S.H., Elesh, Eman, 2014. Temperature and frequency dependencies of AC and dielectric characterizations of copper tetraphenyl porphyrin thin films. Vacuum 99, 153–159.
Flamigni, Lucia, Talarico, Anna Maria, Ventura, Barbara, Rein, Regis, Solladié, Nathalie, 2006. A versatile bis-porphyrin tweezer host for the assembly of noncovalent photoactive architectures: a photophysical characterization of the tweezers and their association with porphyrins and other guests. Chem. Eur. J. 12 (3), 701–712.
Gouterman, Martin, 1959. Study of the effects of substitution on the absorption spectra of porphin. J. Chem. Phys. 30 (5), 1139–1161.
Haque, Ashanul, Faizi, Md. Serajul Haque, Rather, Jahangir Ahmad, Khan, Muhammad S., 2017. Next generation NIR fluorophores for tumor imaging and fluorescence-guided surgery: a review. Bioorg. Med. Chem. 25 (7), 2017–2034.
Haque, Ashanul, Al-Balushi, Rayya A., Al-Busaidi, Idris Juma, Khan, Muhammad S., Raithby, Paul R., 2018. Rise of conjugated poly-ynes and poly(metalla-ynes): from design through synthesis to structure-property relationships and applications. Chem. Rev. 118 (18), 8474–8597.
Hoard, J., Smith, K., 1975. Porphyrins and Metalloporphyrins, by KM Smith. Elsevier, Amsterdam, p. 317.
Imahori, Hiroshi, Umeyama, Tomokazu, Ito, Seigo, 2009. Large π-aromatic molecules as potential sensitizers for highly efficient dye-sensitized solar cells. Acc. Chem. Res. 42 (11), 1809–1818.

Jusélius, Jonas, Sundholm, Dage, 2000. The aromatic pathways of porphins, chlorins and bacteriochlorins. PCCP 2 (10), 2145–2151.
Jentzen, Walter, Ma, Jian-Guo, Shelnutt, John A., 1998. Conservation of the conformation of the porphyrin macrocycle in hemoproteins. J. Biophys. 74 (2), 753–763.
Kim, D., Shin, E.J., 2003. Noncovalently linked zinc porphyrin-Ru (bpy)~ 3 dyad assembled via axial coordination. Bull. Korean Chem. Soc. 24, 1490–1494.
Lu, Hua, Kobayashi, Nagao, 2016. Optically active porphyrin and phthalocyanine systems. Chem. Rev. 116 (10), 6184–6261.
Lind, Samuel J., Gordon, Keith C., Gambhir, Sanjeev, Officer, David L., 2009. A spectroscopic and DFT study of thiophene-substituted metalloporphyrins as dye-sensitized solar cell dyes. PCCP 11 (27), 5598. https://doi.org/10.1039/b900988d.
Lin, Chia-ling, Fang, May-Yang, Cheng, Shu-Hua, 2002. Substituent and axial ligand effects on the electrochemistry of zinc porphyrins. J. Electroanal. Chem. 531 (2), 155–162.
Nath, Ipsita, Chakraborty, Jeet, Verpoort, Francis, 2016. Metal organic frameworks mimicking natural enzymes: a structural and functional analogy. Chem. Soc. Rev. 45 (15), 4127–4170.
Oxford Diffraction, 2010. CrysAlis PRO, CrysAlis CCD and CrysAlis RED. Oxford. Diffraction Ltd, Yarnton, Oxfordshire, England.
Oberda, Krzysztof, Deperasińska, Irena, Nizhnik, Yakov P., Szemik-Hojniak, Anna, 2013. A novel complex of zinc tetraphenylporphyrin with two dioxane molecules in a rare attachment. Crystal structure, spectroscopy and theoretical calculations. Polyhedron 51, 61–69.
Park, Jun Hong, Royer, James E., Chagarov, Evgeniy, Kaufman-Osborn, Tobin, Edmonds, Mary, Kent, Tyler, Lee, Sangyeob, Trogler, William C., Kummel, Andrew C., 2013. Atomic imaging of the irreversible sensing mechanism of NO2 adsorption on copper phthalocyanine. J. Am. Chem. Soc. 135 (39), 14600–14609.
Paul, Dharam, Melin, Frédéric, Hirtz, Caroline, Wytko, Jennifer, Ochsenbein, Philippe, Bonin, Michel, Schenk, Kurt, Maltese, Patrick, Weiss, Jean, 2003. Induced fit process in the selective distal binding of imidazoles in zinc (II) porphyrin receptors. Inorg. Chem. 42 (12), 3779–3787.
Polat, O., Caglar, M., Coskun, F.M., Coskun, M., Caglar, Y., Turut, A., 2020. An investigation of the optical properties of YbFe1-xIrxO3- (x=0, 0.01 and 0.10) orthoferrite films. Vacuum 173, 109124.
Scheidt, W.R., Lee, Y.J., 1987. Recent advances in the stereochemistry of metallotetrapyrroles. Struct. Bonding (Berlin) 64, 1–7.
Soury, Raoudha, Jabli, Mahjoub, Saleh, Tawfik A., Abdul-Hassan, Wathiq Sattar, Saint-Aman, Eric, Loiseau, Frédérique, Philouze, Christian, Nasri, Habib, 2018a. Tetrakis(ethyl-4(4-butyryl)oxyphenyl)porphyrinato zinc complexes with 4,4'-bpyridin: synthesis, characterization, and itscatalyticdegradation of Calmagite. RSC. Adv. 8 (36), 20143–20156.
Soury, Raoudha, Chaabene, Marwa, Jabli, Mahjoub, Saleh, Tawfik A., Ben Chaabane, Rafik, Saint-Aman, Eric, Loiseau, Frédérique, Philouze, Christain, Allouche, Abdul-Rahman, Nasri, Habib, 2019. Meso-tetrakis (3, 4, 5- trimethoxyphenyl) porphyrin derivatives: Synthesis, spectroscopic characterizations and adsorption of NO2. Chem. Eng. J. 375, 122005. https://doi.org/10.1016/j.cej.2019.122005.
Soury, Raoudha, Jabli, Mahjoub, Saleh, Tawfik A., Abdul-Hassan, Wathiq Sattar, Saint-Aman, Eric, Loiseau, Frédérique, Philouze, Christian, Bujacz, Anna, Nasri, Habib, 2018b. Synthesis of the (4, 4′-bipyridine)(5, 10, 15, 20-tetratolylphenylporphyrinato) zinc (II) bis (4, 4-bipyridine) disolvate dehydrate and evaluation of its interaction with organic dyes. J. Mol. Liq. 264, 134–142.
Sommer, Jonathan R., Shelton, Abigail H., Parthasarathy, Anand, Ghiviriga, Ion, Reynolds, John R., Schanze, Kirk S., 2011. Photophysical properties of near-infrared phosphorescent π- extended platinum porphyrins. Chem. Mater. 23 (24), 5296–5304.
Sheldrick, George M., 2008. A short history of SHELX. Acta Crystallogr. Sect. A 64 (1), 112–122.
Sharma, Shalu, Kumar, Manoj, Chhoker, Sandeep, 2019. Parameters dependent synthesis of zinc stannate nanowires using CVD and its porphyrin dye loaded optical studies. Vacuum 161, 201–208.
Tauc, J., Grigorovici, R., Vancu, A., 1966. Optical properties and electronic structure of amorphous germanium. Phys. Stat. Sol. 15 (2), 627–637.
Yang, S.I., Seth, J., Strachan, J.P., Gentemann, S., Dewey, D.K., Lindsey, J.S., Bocian, D. F., 1999. J. Porphyrins. Phthalocyanines 3, 117–147.